# Intestinal Tropism of a Betacoronavirus (*Merbecovirus*) in Nathusius's Pipistrelle Bat (*Pipistrellus nathusii*), Its Natural Host

Vera C. Mols,[a] Mart M. Lamers,[a] Lonneke ME. Leijten,[a] Tim I. Breugem,[a] Marco WG. van de Bildt,[a] Petra B. van den Doel,[a] Peter HC. Lina,[b] Marion PG. Koopmans,[a,c] Bart L. Haagmans,[a] Thijs Kuiken,[a] Lineke Begeman[a]

aDepartment of Viroscience, Erasmus University Medical Center, Rotterdam, The Netherlands
bDepartment of Terrestrial Zoology, Naturalis Biodiversity Center, Leiden, The Netherlands
cPandemic and Disaster Preparedness Centre, Erasmus University Medical Center, Rotterdam, The Netherlands

**ABSTRACT** The emergence of several bat coronavirus-related disease outbreaks in human and domestic animals has fueled surveillance of coronaviruses in bats worldwide. However, little is known about how these viruses interact with their natural hosts. We demonstrate a *Betacoronavirus* (subgenus *Merbecovirus*), PN-$\beta$CoV, in the intestine of its natural host, Nathusius's Pipistrelle Bat (*Pipistrellus nathusii),* by combining molecular and microscopy techniques. Eighty-eight *P. nathusii* bat carcasses were tested for PN-$\beta$CoV RNA by RT-qPCR, of which 25 bats (28%) tested positive. PN-$\beta$CoV RNA was more often detected in samples of the intestinal tract than in other sample types. In addition, viral RNA loads were higher in intestinal samples compared to other sample types, both on average and in each individual bat. In one bat, we demonstrated *Merbecovirus* antigen and PN-$\beta$CoV RNA expression in intestinal epithelium and the underlying connective tissue using immunohistochemistry and *in situ* hybridization, respectively. These results indicate that PN-$\beta$CoV has a tropism for the intestinal epithelium of its natural host, Nathusius's Pipistrelle Bat, and imply that the fecal-oral route is a possible route of transmission.

**IMPORTANCE** Virtually all mammal species circulate coronaviruses. Most of these viruses will infect one host species; however, coronaviruses are known to include species that can infect multiple hosts, for example the well-known virus that caused a pandemic, SARS-CoV-2. Chiroptera (bats) include over 1,400 different species, which are expected to harbor a great variety of coronaviruses. However, we know very little about how any of these coronaviruses interact with their bat hosts; for example, we do not know their modes of transmissions, or which cells they infect. Thus, we have a limited understanding of coronavirus infections in this important host group. The significance of our study is that we learned that a bat coronavirus that occurs in a common bat species in Europe has a tropism for the intestines. This implies the fecal-oral route is a likely transmission route.

Several coronaviruses (CoVs), including severe acute respiratory syndrome CoV type 1 (SARS-CoV-1), Middle East respiratory syndrome CoV (MERS-CoV), severe acute respiratory syndrome CoV type 2 (SARS-CoV-2), and swine acute diarrhea syndrome CoV (SADS-CoV) have caused notable disease outbreaks in humans and animals over the last 20 years (1, 2). Phylogenetic analyses suggest that these viruses originated, at least partly, from bat CoVs (3–6), which likely spilled over from bats to humans and pigs, either directly or through an intermediate host (3, 7, 8). Bats are the second largest order of mammals, comprising approximately 20% of all mammalian species (9, 10). The number of zoonotic viruses originating from this large mammalian order is proportional to the number of different species it is comprised of (11). When bats are sampled and tested, coronaviruses are frequently

detected, suggesting bats are suitable hosts for coronaviruses (7, 12–21). Bat coronaviruses that have been detected belong to the *Alphacoronavirus* and *Betacoronavirus* genera, two of the four genera within the *Coronaviridae* family. Phylogenetics of bat coronaviruses seem to follow the phylogenetics of bat species, suggesting virus-host coevolution (22). Currently there is little known about what characteristics make bat coronaviruses more likely to cross the species barrier and transmit outside their normal bat species host.

The tropism of bat coronaviruses is largely unknown. Tropism for the intestinal tract has been suggested based on the high rate of RNA detection in fecal samples and intestinal tissues (7, 12, 23–26). However, detection of viral RNA in feces does not necessarily prove that the intestinal tract is the primary replication site. For example, RNA of human influenza virus and bat lyssavirus type 1 also can be detected in feces, even though their primary replication sites are the respiratory tract and nervous system, respectively (27, 28). Bat coronavirus RNA has also been detected in upper and lower respiratory tract samples of bats (29, 30). A bat coronavirus found in a naturally infected, captive Little Brown Bat (*Myotis lucifugus*) colony shows tropism for the respiratory tract, more specifically in bronchial epithelial cells (31). In humans, for which coronavirus infections are relatively well studied, coronaviruses can show a tropism for both the upper and lower respiratory tract as well as the intestinal tract (32, 33). In mice, mouse hepatitis virus has a tropism for the liver, nervous tissue, intestinal tract, and lower respiratory tract, depending on the virus strain (34, 35). In livestock and companion animals, coronaviruses commonly cause infections in the respiratory or digestive tract, or both (32, 36–38). Of these, feline enteric CoV, as well as ferret enteric CoV, which replicate predominantly in the intestinal tract, specifically in the intestinal epithelium, can mutate into variants with tropism for the immune system, specifically in macrophages (39, 40), causing systemic infections (41). Given the diversity of CoV tropism in above species, a similar diversity may be expected for the tropism of bat CoVs in their chiropteran hosts.

Bats have been identified as ancestral hosts for epidemic, newly emerging human, and domestic animal coronaviruses. However, determinants of spillover probability and pathways from bat CoVs to other species are largely unknown. Viral dynamics, such as tissue tropism within a reservoir host, are important contributing factors to external shedding and consequently mode of exposure to susceptible animals (42). To better understand the tissue tropism of coronaviruses in bats, our study aimed to investigate the tissue tropism of a $\beta$-CoV regularly detected in Nathusius's Pipistrelle Bats *(Pipistrellus nathusii)* (L. Begeman), a bat species commonly found in the Netherlands (43). This virus, PN-$\beta$CoV (subgenus *Merbecoviruses*, previously known as lineage 2c), has been previously detected by others in Pipistrelle Bats (44, 45).

## RESULTS

**Detection and quantification of PN-$\beta$CoV RNA in bats.** Overall, 28% (25 of 88) of bats tested positive for PN-$\beta$CoV RNA. RNA was detected in intestinal tissues of 21 of 83 (25%) bats for which it was available, in rectal swabs of 16 of 88 (18%) bats, in nose washes of 3 of 37 (8%) bats for which it was available, and in the lungs of 3 of 79 (3%) bats for which it was available (Supplement S1). The percentage of bats testing positive was significantly higher for bats that were necropsied directly after death (8 of 11 bats, 73% positive), compared to bats necropsied after a period of storage at −20°C (17 of 73 bats, 23% positive, $\chi^2$, $P < 0.001$, Table 1).

The majority of bats (15 of 25, 60%) tested PN-$\beta$CoV RNA positive in exclusively intestinal samples. We did not detect bats that were positive in only the respiratory tract samples. In addition, intestinal samples tested positive more frequently compared to any other sample origin (57 to 79% compared to 4 to 20% respiratory sample types and 12 to 16% other sample types, Table 2). Furthermore, higher levels of viral RNA (mean *Ct* values of 25 to 28) were detected in intestinal sample types compared to all other sample types (mean *Ct* values of 30 to 34). Still, all other, nonintestinal sample types included in our analyses had one or more positives, with *Ct* values ranging from 23 (kidney) to 37 (also kidney) (Table 2).

**TABLE 1** Comparison of detection rates and RNA loads detected by RT-qPCR targeting a 154 bp fragment of *Merbecovirus* UpE gene in intestinal tissue, stored dry or in RNAlater (RL), and in rectal swabs, lung tissues and nose wash specimens of bat carcasses necropsied shortly after death versus bat carcasses frozen prior to necropsy

| Group | Intestine (dry) Percentage positive (no. positive/ total) | Mean $Ct \pm SD$ | Intestine (RL) Percentage positive (no. positive/ total) | Mean $Ct \pm SD$ | Rectal swab Percentage positive (no. positive/ total) | Mean $Ct \pm SD$ | Lung Percentage positive (no. positive/ total) | Mean $Ct \pm SD$ | Nose wash Percentage positive (no. positive/ total) | Mean $Ct \pm SD$ |
|---|---|---|---|---|---|---|---|---|---|---|
| Frozen ($n = 74$) | 18% (9/49) | 28 ± 4.45 | 26% (12/46) | 30 ± 3.83 | 14% (10/74) | 28 ± 3.68 | 4% (3/68) | 33 ± 2.63 | 7% (2/27) | 34 ± 2.60 |
| Fresh ($n = 14$) | 60% (6/10) | 27 ± 5.34 | 50% (3/6) | 23 ± 5.50 | 43% (6/14)[a] | 28 ± 3.94 | 0% (6/11) | NA[b] | 10% (1/10) | 32 ± 0 |
| Combined ($n = 88$) | 25% (15/59) | 28 ± 4.65 | 29% (15/52) | 28 ± 4.75 | 18% (16/88)[a] | 28 ± 3.65 | 4% (3/79) | 33 ± 2.63 | 8% (3/37) | 33 ± 2.21 |

[a]No intestinal tissue was available for virological analysis in 5 bats, one of which tested positive in rectal swab. The other four were excluded from further analysis.
[b]NA, not applicable.

The following bivariate statistical analyses to test for a relation between a positive *Merbecovirus* outcome and sex, do not include four bats from which no intestinal tissue was available. Bats included in this study consisted of 66 (79%) males and 18 (21%) females. Detection of PN-$\beta$CoV RNA was not significantly different between males (30%, 20 of 66 positive) and females (28%, 5 of 18 positive) ($\chi^2$, $P = 0.835$). Because our results showed a significantly higher percentage of bats testing positive when in bats necropsied shortly after death compared to bats necropsied after storage at −20℃, sex bias was also tested in the two groups separately. Again, no significant differences were detected between males and females in either of those groups (frozen stored: males 25%, 14 of 57 positive; females 19%, 3 of 16 positive; $\chi^2$, $P = 0.627$; direct necropsy: males 67%, 6 of 9 positive; females 100%, 2 of 2 positive; $\chi^2$, $P = 0.338$).
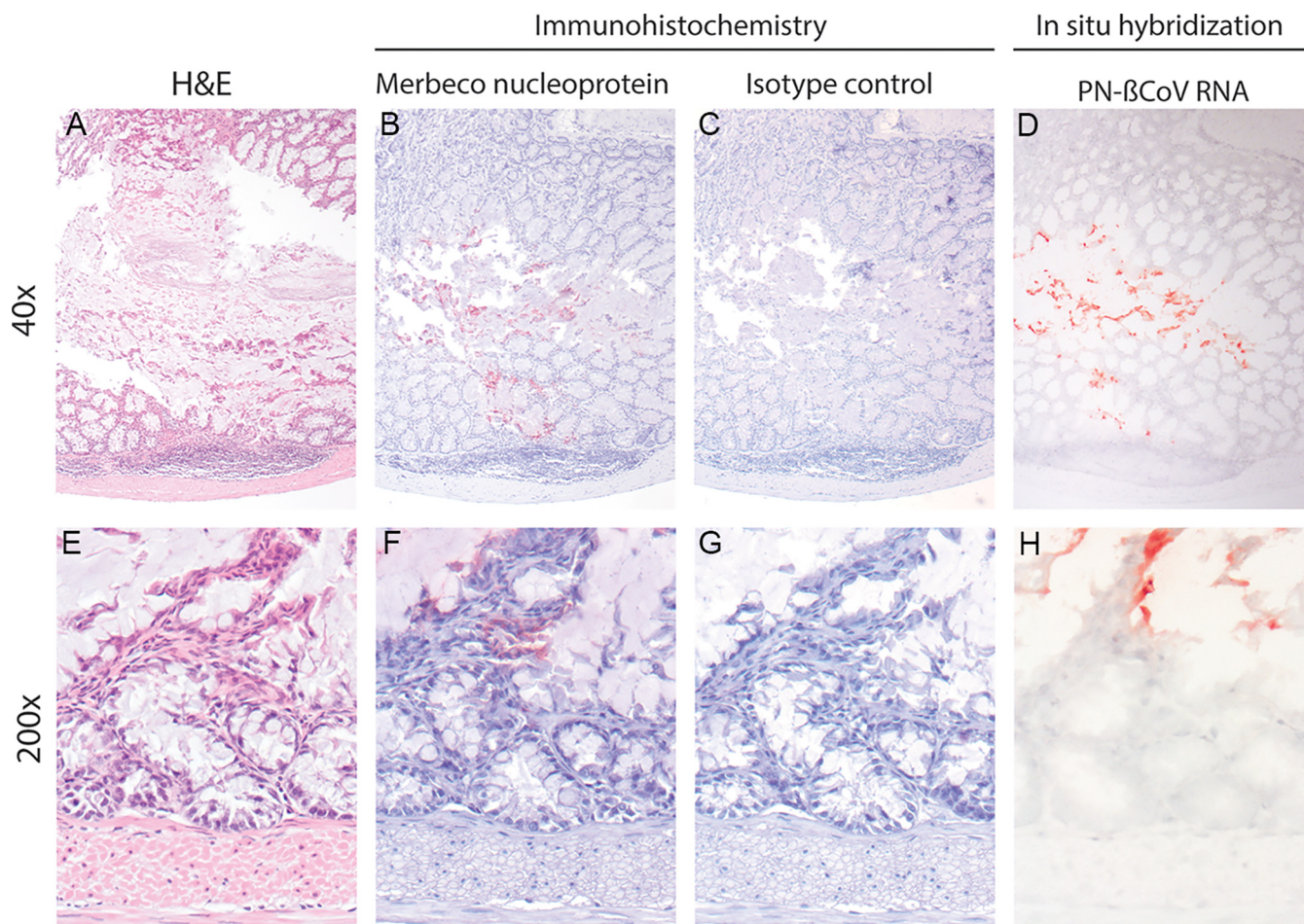
**Phylogenetic analysis.** *Rdrp* fragments of 395 to 396 nt in length were obtained from samples of 13 RT-qPCR-positive bats, as well as a 359 and 383 nt *Rdrp* fragment from two other RT-qPCR-positive bats (Supplement S2). Obtained 395 to 396 nt of *Rdrp* fragments showed a sequence similarity of 96.7 to 100% among one another. Phylogenetic analysis showed that PN-$\beta$CoV clustered with other previously detected *Merbecoviruses* (Fig. 1) in *Pipistrellus* species found in The Netherlands, Romania, Ukraine, and Russia (Supplement S3), with a sequence similarity of ≥97%.

**Immunohistochemistry and *in situ* hybridization.** Of 23 viral RNA positive bats with sufficiently fresh tissue to allow histological analysis, 1 bat expressed viral antigen

**TABLE 2** Proportion *Merbecovirus* positives per sample type in *Merbecovirus*-positive bats, and RNA loads detected by RT-qPCR. Totals indicate the total number of bats positive in at least one sample within a group of sample types

| Sample type | Percentage positive (no. positive/total) | Mean $Ct$ value (range) |
|---|---|---|
| Intestinal | | |
|   RNAlater intestine | 79% (15/19) | 28 (18–36) |
|   Dry intestine | 63% (15/24) | 28 (20–37) |
|   Rectal swab | 64% (16/25) | 28 (23–33) |
|   Feces | 57% (12/21) | 25 (17–35) |
|   **Total** | 100% (25/25) | |
| | | |
| Respiratory | | |
|   Nose wash | 20% (3/15) | 33 (32–36) |
|   Lung | 12% (3/25) | 33 (31–36) |
|   Oral swab | 4% (1/25) | 31 (31) |
|   **Total** | 16% (4/25) | |
| | | |
| Other | | |
|   Liver | 16% (4/25) | 30 (24–33) |
|   Kidney | 16% (4/25) | 32 (23–37) |
|   Brain | 16% (4/25) | 34 (32–35) |
|   Spleen | 12% (3/25) | 33 (28–36) |

**FIG 1** RNA-dependent RNA polymerase-based phylogeny of novel sequences and reference *Betacoronaviruses* obtained from GenBank based on 338–396 nt fragments corresponding to positions 15353 to 15747 in Middle East respiratory syndrome-related coronavirus isolate Bat-CoV/P.nathusii/Russia/MOW15-22/2015 (GenBank accession no. ON325306). Phylogenetically distinct PN-$\beta$CoV sequences obtained in this study are displayed in bold. Reference sequences of *Betacoronaviruses* classified within subgenera Sarbecovirus, Embecovirus and Nobecovirus are collapsed. Accession numbers available in Supplement S2 and S3.

in cells within the intestine (Fig. 2). In all other tissues of this bat, and all tissues of the other 22 bats, viral antigen was not detected. Tissues from 2 of 25 PN-$\beta$CoV RNA-positive bats showed advanced autolysis of the epithelium and were excluded from IHC staining.

In the one viral antigen positive bat, antigen was expressed as variably sized, indistinctly delineated granules within cytoplasm of both individual cells and clusters of cells, which displayed a morphology consistent with mucus producing cells. In addition, scattered, individual cells in the connective tissue (lamina propria) between the intestinal crypts (Fig. 2 and 3) stained similarly positive. The cells expressing viral antigen within the lamina propria were difficult to identify based on morphology and could either be fibroblasts or immune cells. The isotype control to test for aspecific binding was negative. There was no inflammation or other lesions that colocalized with the viral antigen expression.

*In situ* hybridization on serial sections of this intestinal sample expressing viral antigen showed PN-$\beta$CoV RNA expression in the same region where there was viral antigen expression. Viral RNA was visible as bright pink granules in the same area that expressed viral antigen (Fig. 2). Comparison of the viral RT-qPCR results of this bat with those of the viral antigen negative bats showed that viral loads were higher, especially in the intestinal samples: $Ct$ 18 in intestine stored in RNAlater, compared to average $Ct$ of 28 (range 18 to 36); $Ct$ 19 in feces compared to 25 (range 17 to 35); $Ct$ 23 in dry intestine compared to 28 (range 20 to 37); and $Ct$ 26 in rectal swab compared to 28 (range

**FIG 2** Histology, PN-$\beta$CoV viral antigen expression and PN-$\beta$CoV viral RNA expression at two magnifications, in the intestinal mucosa of a Nathusius's Pipistrelle Bat. (A) Intestine with lumen in the center and epithelium on top and bottom, lined by lamina propria, muscular wall and serosa on the bottom. The lamina propria is expanded by densely cellular gastrointestinal lymphoid tissue. Epithelium nearest to the lumen is sloughed off due to autolysis, while more toward the serosa epithelial architecture has been preserved. H&E. (B) PN-$\beta$CoV antigen expression, visible as red staining, in a distinct intestinal epithelial area that extends from the center (lumen side) to the bottom of the panel (serosa side). IHC with MERS-CoV nucleoprotein antibody which shows cross-reactivity with PN-$\beta$CoV, developed with AEC. (C) Isotype control shows no staining. Serial section, isotype control with anti-mouse IgG1. (D) Expression of PN-$\beta$CoV RNA is present as red staining in the same area staining positive for PN-$\beta$CoV antigen. Serial section, ISH for PN-$\beta$CoV RNA. (E) Higher magnification of intestinal mucosa at another location than shown in (A) to (D), with epithelial layer containing crypts embedded in connective tissue (lamina propria) on top and muscular layer on the bottom of the panel. No pathological changes, such as infiltration of immune cells or necrosis. Mild autolysis at the base of the crypts, progressing to moderate autolysis toward the top of the panel. H&E. (F) PN-$\beta$CoV antigen is present as dark red granules in cells within intestinal lamina propria and throughout the cytoplasm of epithelial cells. Serial section, IHC with MERS-CoV nucleoprotein antibody which shows cross-reactivity with PN-$\beta$CoV, developed with AEC. (G) Isotype control shows no staining. Serial section, isotype control with anti-mouse IgG1. (H) Expression of PN-$\beta$CoV RNA is present as red staining in the same area that expresses PN-$\beta$CoV antigen. The histological details are faint due to the harsh treatment of the tissue section for ISH. Serial section, ISH for PN-$\beta$CoV RNA.

23 to 33). The other (IHC negative) tissues of this bat had $Ct$ values of 23 (kidney), 24 (liver), and 28 (spleen). Supplement S1 provides RT-qPCR results for each individual positive bat.

## DISCUSSION

By the demonstration of expression of viral antigen and PN-$\beta$CoV RNA in epithelial cells and cells within the lamina propria of the intestine of one bat, we show PN-$\beta$CoV has intestinal tropism in its natural bat host, Nathusius's Pipistrelle Bat. Our results suggest these cells are a replication site for this virus and a likely source for the viral RNA detected in feces and rectal swabs of other bats in this study. The detection of higher viral RNA loads in intestinal samples compared to any other sample type in all positive bats support this. Based on morphology virus positive cells in the intestinal epithelium included mucus-producing cells, and those in the lamina propria were either fibroblasts or immune cells. Further characterization of these cell types would increase our understanding of this virus infection in Nathusius's Pipistrelle Bats.
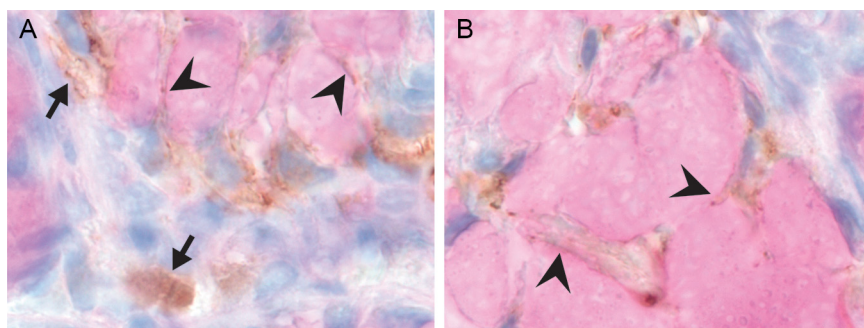
**FIG 3** PN-βCoV antigen expression in the intestine. Arrowheads indicate brown virus-antigen staining that based on localization and morphology is consistent to be in cytoplasm of mucus-cells. Mucus-cells are characterized by a basal, somewhat flattened nucleus, and a thin layer of cytoplasm that surrounds a purple globule (mucus). Arrows indicate brown virus staining of cells in the connective tissue bordering crypts (lamina propria), potentially fibroblasts, or immune cells (×1000 magnification, PN-βCoV IHC developed with DAB, with PAS counterstain to highlight mucus inside mucus-cells).

While we detected intestinal tract tropism for PN-βCoV in our Nathusius's Pipistrelle Bats, others have detected a bat coronavirus that had respiratory tract tropism in its natural bat hosts. In that study 'Myl-CoV' RNA, was somewhat similar to our results detected in intestinal tissues of a high percentage (53 of 174, 30%) of Little Brown Bats, and for a much smaller percentage in lungs (5 of 174, 3%). In that study, however, only lung sections expressed coronavirus antigen by IHC, and not sections of the intestinal tract. In the lungs, bronchial epithelial cells specifically stained positive for virus antigen, and the presence of virus particles in these cells was confirmed by electron microscopy (31). Coronavirus infections in other mammals, like humans and cattle, have shown that coronaviruses can have a tropism for the respiratory tract as well as the intestinal tract in a single host species (33). Future studies of coronaviral tropism in infected bats will help to understand if the PN-βCoV in Nathusius's Pipistrelle Bats has additional tropism for cells outside the gastrointestinal tract.

Coronavirus tropism is highly dependent on the presence and distribution of cellular receptors (46–48). The cellular receptors used by PN-βCoV are currently unknown. However, *in silico* and phylogenetic analysis suggests that this virus might have affinity for bat DPP4 (49). DPP4 expression has been demonstrated in epithelial cells of the intestinal tract, but not in the respiratory tract, in a species closely related to Nathusius's Pipistrelle Bats (50). This suggests that coronaviruses that use DPP4 will have an intestinal tropism in these bats.

Our findings indicate intestinal tropism; however, several other intestine samples tested positive by RT-qPCR yet showed no viral antigen expression by IHC. A possible explanation is that the IHC is not very sensitive. However, the overlap in staining area of the PN-βCoV ISH and virus IHC, together with the known high sensitivity of *in situ* hybridization technique (51), contradicts this. A possible explanation for these results is that our virus IHC was less sensitive than our viral RT-qPCR, so that only cells at their peak of virus production could be detected. Alternatively, the amount of intestine in the slides might not have been big enough to detect a small number of infected cells with IHC. Another explanation is that viral RNA can persist long after viral infection has been cleared. Similarly, it has been observed that SARS-CoV-2 infected patients can remain PCR positive up to months after disease recovery. Many of these PCR positive patients that do not show clinical signs of COVID19 are culture negative and do not transmit SARS-CoV-2; nor does SARS-CoV-2 infection reemerge later (52–54), suggesting that they cleared their infection, while viral RNA remains detectable in their samples for some time. For SARS-CoV-2 infection and likely other virus infections, another determinant of virus infection, besides detection of antigen positive cells, is the detection of high viral loads by quantitative PCR (55). In our study the intestine sample in which we detected virus antigen had the highest viral load measured by quantitative PCR. This suggests that, for future studies into bat

coronavirus infection, quantitative viral PCRs are a helpful tool to add to the currently commonly performed qualitative viral PCRs.

To conclude, PN-$\beta$CoV was detected in epithelial cells of the intestine in its natural host, Nathusius's Pipistrelle Bat, suggesting this is a replication site for the virus. The fecal-oral route therefore represents a likely transmission route among bats of this species. Revealing intestines as a site of virus replication will help to focus future efforts to culture PN-$\beta$CoV, to understand its pathogenesis, and to understand transmission of the virus between bats.

## MATERIALS AND METHODS

**Study setup.** The study was embedded in a bat mortality screening program further described below. To investigate the tropism of a coronavirus-bat host pair, we chose a $\beta$-CoV that we detected in naturally infected Nathusius's Pipistrelle Bats. We chose a $\beta$-CoV because previously recognized promiscuous, less species-specific coronaviruses like SARS-CoVs, MERS-CoV, and bovine coronavirus belong to this genus (56), and we chose Nathusius's Pipistrelle Bats because carcasses of naturally infected bats were available to us, and because it is one of the most common synanthropic bat species in the Netherlands, mainly from mid-August until mid-May. From mid-May until mid-August, the majority of the population consist of males, and females are almost absent. In late summer and early autumn, there is an influx of large numbers of adult and subadult females into the Netherlands to join territorial males to mate (43). First, we identified carcasses for the presence of *P. nathusii* $\beta$-CoV (PN-$\beta$CoV) RNA by investigating intestinal and respiratory samples using a RT-qPCR set up for the detection of this *Merbecovirus*. Intestinal samples have proven to be a sensitive sample to detect viruses with varied tropism, including respiratory (28), neurologic (27), and intestinal tropism (57). Next, a standard set of samples from each positive carcass was further investigated by RT-qPCR and immunohistochemistry to localize PN-$\beta$CoV RNA and antigen. This standard set contained all tissues that were available for virology and microscopy in parallel, which were lung, intestine, kidney, brain, liver, and spleen. PN-$\beta$CoV specific *in situ* hybridization was used to confirm IHC-staining specificity. If intracellular virus antigen or viral RNA was detected by staining, colocalization with lesions was examined on serial sections stained with hematoxylin and eosin (H&E).

**Bat sampling and necropsy.** We used carcasses from Nathusius's Pipistrelle Bats that were found dead, or from bats that were euthanized because of poor prognosis for survival and release, based on evaluation by bat rehabilitators in rehabilitation centers across the Netherlands. These bat carcasses were routinely frozen at −20°C until the date of transport to our facility and subsequent necropsy. Transport and investigation were performed under permit FF/75A/2015/036 from the Dutch Ministry of Economic Affairs. In response to the initiation of this project, a request was made to a local rehabilitation center to also immediately notify the researchers if a Nathusius's Pipistrelle Bat in their care had died. These bats were then necropsied as soon as possible, in order to obtain non-frozen tissues in addition to the tissues of the frozen carcasses. For this study, all 88 Nathusius's Pipistrelle Bat carcasses collected between 2016 and 2021 were selected. Of these, 74 had been stored at −20°C between 1 and 23 months prior to necropsy, and 14 had been necropsied within 6 h postmortem. Species of each bat was determined by an experienced bat researcher (PHCL) using phenotypic characteristics, and later confirmed by DNA analysis.

Necropsies were performed according to standard protocol at biosafety level 2. Samples collected for virology and microscopy in parallel were lung, intestine, kidney, brain, liver, and spleen. Additionally, rectal and pharyngeal swab specimens and, if present, feces from the rectum, were collected for virological analysis and were each stored in 1 mL virus transport medium (VTM) made according to an existing protocol (58). Nasal washes were performed for a subset of carcasses, arbitrarily selected. For this, 500 $\mu$L VTM was gently inserted into one of the choana, and then collected when dripping from the nostrils. For virology, samples were stored at −80°C, or in RNAlater (4°C for 24 h to fixate, −20°C storage). For microscopy, samples were fixed in formalin and paraffin embedded. These included small pieces of lung, brain, kidney, liver and spleen. Complete intestines were embedded, except for a centimeter distal segment that was collected for virology. Skulls were fixed in formalin, then decalcified in 10% EDTA before dehydration and embedding in paraffin in the sagittal plane in order to get a good view on the entire nose.

**Molecular confirmation of bat species.** For confirmation of the bat species via DNA analysis, liver tissue from each bat was homogenized in 1 mL VTM using a 1/4" ceramic sphere (MP Biomedicals). DNA was extracted from 200 $\mu$L homogenate using a QIAamp DNA minikit (Qiagen) in accordance with the manufacturer's instructions and eluted in 200 $\mu$L buffer AE provided in the kit. 5 $\mu$L eluted DNA was added to a PCR mix containing 0.75 $\mu$L (each) of 10 $\mu$M primers (Fwd primer SFF_145: 5′ GTHACHGCYCAYGCHTTYGTAATAAT 3′, Rv primer SFF_351r: 5′ CTCCWGCRTGDGCWAGRTTTCC 3′) targeting a 202 nt fragment of mitochondrial gene cyto-chrome c oxidase subunit I (COI) (59), 0.75 $\mu$L 10 mM deoxynucleoside triphosphates, 2.5 $\mu$L 10× PfuUltra II Rxn buffer (Agilent), 0.5 $\mu$L PfuUltra II fusion HS DNA polymerase (Agilent), 0.5 $\mu$L dimethyl sulfoxide (Sigma-Aldrich), and 14.25 $\mu$L MilliQ water. Amplification was performed in a C1000 Touch Thermal Cycler (Bio-Rad) using the following program: 3 min at 95°C, 40 cycles of 30 s at 95°C, 30 s at 48°C and 40 s at 72°C, and a final extension step of 10 min at 72°C. 5 $\mu$L PCR product was reamplified using the same PCR mix and program.

The second-round PCR products were run on a 2% agarose gel with SYBR Safe DNA Gel Stain (Invitrogen) and visualized using a ChemiDoc MP imaging system (Bio-Rad). Bands with the expected size of ~202 nt were excised on a UVP Visi-Blue Transilluminator and stored at −20°C until further processing.

DNA was extracted from excised bands using a QIAquick Gel Extraction kit (Qiagen) in accordance with the manufacturer's instructions and eluted in 10 $\mu$L Buffer EB (10 mM Tris·Cl, pH 8.5) provided in the kit. A sanger sequencing PCR was performed in two 10 $\mu$L reactions (one forward and one reverse per sample)

containing 2 $\mu$L DNA extract, 3 $\mu$L primer (2 pmol/$\mu$L) (forward reaction primer SFF_145, reverse reaction primer SFF_145), 1.75 $\mu$L 5× sequencing buffer (Applied Biosystems), 0.5 $\mu$L BigDye Terminator v3.1 Ready Reaction Mix (Applied Biosystems) and 2.75 $\mu$L MilliQ water. Sanger sequencing PCR was performed in a C1000 Touch Thermal Cycler (Bio-Rad) using the following program: 10 s at 96℃, 30 s at 45℃ and 30 cycles of 4 min at 60℃. Products were analyzed using an Applied Biosystems Hitachi 3130xl Genetic Analyzer (Applied Biosystems). Sequences generated were assembled and trimmed in DNA Baser Assembler v5.15.0 and compared to available sequences in GenBank.

**RT-qPCR.** Primers and a probe were designed using PN-$\beta$CoV (accession no. OQ405399 and OQ405401) and a MERS-CoV reference sequence (accession no. NC_019843.3) to amplify and quantify PN-$\beta$CoV Up-E gene as well as MERS-CoV Up-E gene via RT-qPCR. To evaluate specificity, *in silico* analysis was performed through alignment of various *Merbecovirus* reference sequences as well as UpE gene of an *Alphacoronavirus* detected in *P. nathusii* bats (accession no. OQ405400). Primers were able to bind exclusively to PN-$\beta$CoV and MERS-CoV Up-E genes. RT-qPCR was performed on rectal swabs and intestinal tissue from each bat, as well as lung and nose wash. Intestine in RNAlater was washed in PBS and homogenized in 1 mL VTM using a 1/4" ceramic sphere (MP Biomedicals). Intestine stored without medium was used if intestine in RNAlater was not available. Total nucleic acids were isolated from 60 $\mu$L rectal swab suspension and 60 $\mu$L intestine homogenate supernatant via a previously in-house developed method using magnetic beads (AMPure XP, Beckman Coulter) and MagNA Pure 96 External Lysis Buffer (Roche) (60) and eluted into 30 $\mu$L elution buffer (Roche). Three $\mu$L of a known concentration of PDV was added to the lysis buffer as internal control; 5 $\mu$L RNA extract was added to 15 $\mu$L RT-qPCR mix targeting a 154 bp fragment of virus UpE gene containing 0.5 $\mu$L of 10 $\mu$M concentrations of Fwd primer (5'-CCTGCAACGCGCGAT-3'), Rv primer (5'-TGGACAAAGGGTAACATAGTTCG-3') and probe (5' FAM-TGGATTAGCCTCTACACGGGACCCATAG-3'), 0.4 $\mu$L PDV primer/probe stock, 5 $\mu$L of TaqMan Fast Virus 1-Step Master Mix (ThermoFisher Scientific), and 8.1 $\mu$L MilliQ water. 5 $\mu$L eluted RNA from MERS-CoV culture supernatant derived from infected human airway organoids, diluted 1:10 in MilliQ water, was used as a positive control. Amplification was performed and detected using the following cycling program on an Applied Biosystems 7500 Real Time PCR System: 5 min at 50℃ and 20 s at 95℃, followed by 40 cycles of 3 s at 950C and 31 s at 60℃. Of all bats in which virus RNA was detected (Ct <40) in intestine, rectal swab, lungs, or nose wash, all other available samples were further tested for PN-$\beta$CoV RNA.

**Coronavirus PCR and sequencing.** In order to obtain viral sequences of partial RNA-dependent RNA polymerase (*Rdrp*) for each RT-qPCR-positive bat, samples with the highest viral RNA load based on the RT-qPCR were further analyzed with a pan-coronavirus PCR as described by (61). Sanger sequencing was performed using a BigDye Terminator Cycle v3.1 kit in accordance with the manufacturer's instructions in an Applied Biosystems Hitachi 3130xl Genetic Analyzer. Assembly was performed using DNA Baser Assembler v5.15.0. Sequences were aligned using ClustalW with reference sequences from GenBank, and a maximum-likelihood tree was obtained using IQ-TREE multicore v1.6.12 and visualized with FigTree v1.4.4.

**Statistical analysis.** Bivariate $X^2$-tests ($P < 0.05$) were performed to exploratively evaluate possible influence of bat sex and carcass storage conditions, namely: on ice for up to 6 h prior to necropsy (fresh) or stored for a period of time at −20℃ (frozen), on PN-$\beta$CoV RNA detection.

**Immunohistochemistry.** *Merbecovirus* immunohistochemistry was performed only on those PN-$\beta$CoV RNA positive bats for which tissues showed minimal autolytic changes (23 of 25) in hematoxylin and eosin (H&E) stained sections. For immunohistochemistry, we used serial, 3-$\mu$m-thick, formalin-fixed, paraffin-embedded sections of all available tissues. Lung tissue derived from a MERS-CoV infected mouse was used as a positive control. Sections were deparaffinized and pretreated by boiling in citric acid buffer (10 mM, pH 6.0) for 15 min. Sections were then washed twice with PBS and endogenous peroxidase was blocked with 3% hydrogen peroxide. After washing with PBS and PBS/Tween, the sections were stained with 5 $\mu$g/mL mouse-anti-HCoV-EMC/2012 nucleoprotein mIgG1 (Sino Biological Inc. Cat No. 44068-MM10) diluted in PBS/0.1% BSA overnight at 4℃. As a negative control, consecutive sections were stained with mouse IgG1 isotype control 1:100 in PBS/0.1% BSA. Slides were washed twice with PBS/Tween and incubated with anti-mIgG1-HRP diluted 1:100 in PBS/0.1% BSA for 1 h at room temperature, then washed twice with PBS. Staining was developed with 5% aminoethyl carbazole (AEC) in DMF and 0.05% $H_2O_2$ in NaAc. Sections were counterstained with Mayer's hematoxylin.

To better visualize morphology of cells in which viral antigen had been detected, the *Merbecovirus* immunohistochemistry protocol described above was repeated on sections of the *Merbecovirus* antigen-positive bat intestine, but with a Periodic acid-Schiff (PAS) counterstain instead of Mayer's hematoxylin. To ensure contrast with the purple-magenta PAS counterstain, the IHC was developed with 3,3'-diaminobenzidine (DAB), which stains brown, instead of the previously used AEC, which stains red. Micrographs were taken with a ZEISS Axiocam 305 color camera attached to a ZEISS Axio Imager.A2 light microscope.

**In situ hybridization.** To confirm specificity of the IHC staining, IHC-positive bat tissues were selected for *in situ* hybridization. ISH was performed on 5 $\mu$m FFPE sections according to manufacturer's instructions for BaseScope. Lung tissue derived from a mouse inoculated with MERS-CoV was used as positive control. A C1 BaseScope (Advanced Cell Diagnostics) probe was custom designed to target a conserved region of PN-$\beta$CoV orf1ab, in addition to MERS orf1ab. Consecutive slides for each section were stained with a DAPB probe (Advanced Cell Diagnostics Cat No. 701011) as negative control. Micrographs were taken using a ZEISS Axiocam 305 color camera attached to a ZEISS Axio Imager.A2 light microscope.

**Data availability.** The PN-$\beta$CoV (partial) genome sequences reported in this study were deposited to GenBank under accession numbers OQ405399 and OQ405401. The *Alphacoronavirus* genome was deposited under accession number OQ405400. The *Rdrp* sequences were deposited under accession numbers OQ348392 to OQ348406.

## REFERENCES

1. Chathappady House NN, Palissery S, Sebastian H. 2021. Corona Viruses: a Review on SARS, MERS and COVID-19. Microbiol Insights 14:117863612110024. https://doi.org/10.1177/11786361211002481.

2. Zhou P, Fan H, Lan T, Yang X-L, Shi W-F, Zhang W, Zhu Y, Zhang Y-W, Xie Q-M, Mani S, Zheng X-S, Li B, Li J-M, Guo H, Pei G-Q, An X-P, Chen J-W, Zhou L, Mai K-J, Wu Z-X, Li D, Anderson DE, Zhang L-B, Li S-Y, Mi Z-Q, He T-T, Cong F, Guo P-J, Huang R, Luo Y, Liu X-L, Chen J, Huang Y, Sun Q, Zhang X-L-L, Wang Y-Y, Xing S-Z, Chen Y-S, Sun Y, Li J, Daszak P, Wang L-F, Shi Z-L, Tong Y-G, Ma J-Y. 2018. Fatal swine acute diarrhoea syndrome caused by an HKU2-related coronavirus of bat origin. Nature 556:255–258. https://doi.org/10.1038/s41586-018-0010-9.

3. Anthony SJ, Gilardi K, Menachery VD, Goldstein T, Ssebide B, Mbabazi R, Navarrete-Macias I, Liang E, Wells H, Hicks A, Petrosov A, Byarugaba DK, Debbink K, Dinnon KH, Scobey T, Randell SH, Yount BL, Cranfield M, Johnson CK, Baric RS, Lipkin WI, Mazet JAK. 2017. Further evidence for bats as the evolutionary source of Middle East respiratory syndrome coronavirus. mBio 8:e00373-17. https://doi.org/10.1128/mBio.00373-17.

4. Huang Y-W, Dickerman AW, Piñeyro P, Li L, Fang L, Kiehne R, Opriessnig T, Meng X-J. 2013. Origin, evolution, and genotyping of emergent porcine epidemic diarrhea virus strains in the United States. mBio 4:00737-13. https://doi.org/10.1128/mBio.00737-13.

5. Li W, Shi Z, Yu M, Ren W, Smith C, Epstein JH, Wang H, Crameri G, Hu Z, Zhang H, Zhang J, McEachern J, Field H, Daszak P, Eaton BT, Zhang S, Wang L-F. 2005. Bats are natural reservoirs of SARS-like coronaviruses. Science 310:676–679. https://doi.org/10.1126/science.1118391.

6. Zhou P, Yang X-L, Wang X-G, Hu B, Zhang L, Zhang W, Si H-R, Zhu Y, Li B, Huang C-L, Chen H-D, Chen J, Luo Y, Guo H, Jiang R-D, Liu M-Q, Chen Y, Shen X-R, Wang X, Zheng X-S, Zhao K, Chen Q-J, Deng F, Liu L-L, Yan B, Zhan F-X, Wang Y-Y, Xiao G-F, Shi Z-L. 2020. A pneumonia outbreak associated with a new coronavirus of probable bat origin. Nature 579:270–273. https://doi.org/10.1038/s41586-020-2012-7.

7. Lau SK, Woo PC, Li KS, Huang Y, Tsoi H-W, Wong BH, Wong SS, Leung S-Y, Chan K-H, Yuen K-Y. 2005. Severe acute respiratory syndrome coronavirus-like virus in Chinese horseshoe bats. Proc Natl Acad Sci USA 102: 14040–14045. https://doi.org/10.1073/pnas.0506735102.

8. Wang Q, Chen H, Shi Y, Hughes AC, Liu WJ, Jiang J, Gao GF, Xue Y, Tong Y. 2021. Tracing the origins of SARS-CoV-2: lessons learned from the past. Cell Res 31:1139–1141. https://doi.org/10.1038/s41422-021-00575-w.

9. Mammal Diversity Database. 2022. Mammal diversity database. https://doi.org/10.5281/ZENODO.6407053.

10. Simmons NB, Cirranello AL. 2022. Bat species of the world: a taxonomic and geographic database. https://doi.org/10.5281/ZENODO.6857865.

11. Mollentze N, Streicker DG. 2020. Viral zoonotic risk is homogenous among taxonomic orders of mammalian and avian reservoir hosts. Proceedings of the National Academy of Sciences 117:9423–9430. https://doi.org/10.1073/pnas.1919176117.

12. Anthony SJ, Ojeda-Flores R, Rico-Chávez O, Navarrete-Macias I, Zambrana-Torrelio CM, Rostal MK, Epstein JH, Tipps T, Liang E, Sanchez-Leon M, Sotomayor-Bonilla J, Aguirre AA, Ávila-Flores R, Medellín RA, Goldstein T, Suzán G, Daszak P, Lipkin WI. 2013. Coronaviruses in bats from Mexico. J General Virology 94: 1028–1038. https://doi.org/10.1099/vir.0.049759-0.

13. Gloza-Rausch F, Anne Ipsen A, Seebens A, Göttsche M, Panning M, Bispo de Filippis AM, Petersen N, Grywna AAK, Müller MA, Pfefferle S, Park SS. 2008. Detection and prevalence patterns of Group I coronaviruses in bats, northern Germany. Emerg Infect Dis 14:626–631. https://doi.org/10.3201/eid1404.071439.

14. Lelli D, Papetti A, Sabelli C, Rosti E, Moreno A, Boniotti M. 2013. Detection of coronaviruses in bats of various species in Italy. Viruses 5:2679–2689. https://doi.org/10.3390/v5112679.

15. Muzeniek T, Perera T, Siriwardana S, Bas D, Kaplan F, Öruc M, Becker-Ziaja B, Schwarz F, Premawansa G, Premawansa S, Perera I, Yapa W, Nitsche A, Kohl C. 2021. Detection of alpha- and betacoronaviruses in *Miniopterus fuliginosus* and *Rousettus leschenaultii*, two species of Sri Lankan bats. Vaccines 9:650. https://doi.org/10.3390/vaccines9060650.

16. Osborne C, Cryan PM, O'Shea TJ, Oko LM, Ndaluka C, Calisher CH, Berglund AD, Klavetter ML, Bowen RA, Holmes KV, Dominguez SR. 2011. Alphacoronaviruses in New World bats: prevalence, persistence, phylogeny, and potential for interaction with humans. PLoS One 6:e19156. https://doi.org/10.1371/journal.pone.0019156.

17. Smith CS, de Jong CE, Meers J, Henning J, Wang L-F, Field HE. 2016. Coronavirus infection and diversity in bats in the Australasian region. Ecohealth 13:72–82. https://doi.org/10.1007/s10393-016-1116-x.

18. Valitutto MT, Aung O, Tun KYN, Vodzak ME, Zimmerman D, Yu JH, Win YT, Maw MT, Thein WZ, Win HH, Dhanota J, Ontiveros V, Smith B, Tremeau-Brevard A, Goldstein T, Johnson CK, Murray S, Mazet J. 2020. Detection of novel coronaviruses in bats in Myanmar. PLoS One 15:e0230802. https://doi.org/10.1371/journal.pone.0230802.

19. Wacharapluesadee S, Duengkae P, Chaiyes A, Kaewpom T, Rodpan A, Yingsakmongkon S, Petcharat S, Phengsakul P, Maneeorn P, Hemachudha T. 2018. Longitudinal study of age-specific pattern of coronavirus infection in Lyle's flying fox (*Pteropus lylei*) in Thailand. Virol J 15:38. https://doi.org/10.1186/s12985-018-0950-6.

20. Watanabe S, Masangkay JS, Nagata N, Morikawa S, Mizutani T, Fukushi S, Alviola P, Omatsu T, Ueda N, Iha K, Taniguchi S, Fujii H, Tsuda S, Endoh M, Kato K, Tohya Y, Kyuwa S, Yoshikawa Y, Akashi H. 2010. Bat coronaviruses

and experimental infection of bats, the Philippines. Emerg Infect Dis 16: 1217–1223. https://doi.org/10.3201/eid1608.100208.

21. Woo PC, Lau SK, Li KS, Poon RW, Wong BH, Tsoi H-w, Yip BC, Huang Y, Chan K-h, Yuen K-y. 2006. Molecular diversity of coronaviruses in bats. Virology 351:180–187. https://doi.org/10.1016/j.virol.2006.02.041.

22. Ruiz-Aravena M, McKee C, Gamble A, Lunn T, Morris A, Snedden CE, Yinda CK, Port JR, Buchholz DW, Yeo YY, Faust C, Jax E, Dee L, Jones DN, Kessler MK, Falvo C, Crowley D, Bharti N, Brook CE, Aguilar HC, Peel AJ, Restif O, Schountz T, Parrish CR, Gurley ES, Lloyd-Smith JO, Hudson PJ, Munster VJ, Plowright RK. 2022. Ecology, evolution and spillover of coronaviruses from bats. In Nat Rev Microbiol 20:299–314. https://doi.org/10.1038/s41579-021-00652-2.

23. Hernández-Aguilar I, Lorenzo C, Santos-Moreno A, Naranjo EJ, Navarrete-Gutiérrez D. 2021. Coronaviruses in bats: a review for the Americas. Viruses 13: 1226. https://doi.org/10.3390/v13071226.

24. Lau SKP, Li KSM, Huang Y, Shek C-T, Tse H, Wang M, Choi GKY, Xu H, Lam CSF, Guo R, Chan K-H, Zheng B-J, Woo PCY, Yuen K-Y. 2010. Ecoepidemiology and Complete Genome Comparison of Different Strains of Severe Acute Respiratory Syndrome-Related Rhinolophus Bat Coronavirus in China Reveal Bats as a Reservoir for Acute, Self-Limiting Infection That Allows Recombination Events. J Virol 84:2808–2819. https://doi.org/10.1128/JVI.02219-09.

25. Pfefferle S, Oppong S, Drexler JF, Gloza-Rausch F, Ipsen A, Seebens A, Müller MA, Annan A, Vallo P, Adu-Sarkodie Y, Kruppa TF, Drosten C. 2009. Distant relatives of severe acute respiratory syndrome coronavirus and close relatives of human coronavirus 229E in bats, Ghana. Emerg Infect Dis 15:1377–1384. https://doi.org/10.3201/eid1509.090224.

26. Tang XC, Zhang JX, Zhang SY, Wang P, Fan XH, Li LF, Li G, Dong BQ, Liu W, Cheung CL, Xu KM, Song WJ, Vijaykrishna D, Poon LLM, Peiris JSM, Smith GJD, Chen H, Guan Y. 2006. Prevalence and genetic diversity of coronaviruses in bats from China. J Virol 80:7481–7490. https://doi.org/10.1128/JVI.00697-06.

27. Begeman L, Kooi EA, Weezep E, Bildt MWG, Reusken CBEM, Lina PHC, Koopmans MPG, Brand JMA, Kuiken T. 2020. Faeces as a novel material to estimate lyssavirus prevalence in bat populations. Zoonoses Public Health 67:198–202. https://doi.org/10.1111/zph.12672.

28. Hirose R, Nakaya T, Naito Y, Daidoji T, Watanabe Y, Yasuda H, Konishi H, Itoh Y. 2017. Mechanism of human influenza virus RNA persistence and virion survival in feces: mucus protects virions from acid and digestive juices. J Infect Dis 216:105–109. https://doi.org/10.1093/infdis/jix224.

29. Bittar C, Machado RRG, Comelis MT, Bueno LM, Beguelini MR, Morielle-Versute E, Nogueira ML, Rahal P. 2020. Alphacoronavirus detection in lungs, liver, and intestines of bats from Brazil. Microb Ecol 79:203–212. https://doi.org/10.1007/s00248-019-01391-x.

30. Poon LLM, Chu DKW, Chan KH, Wong OK, Ellis TM, Leung YHC, Lau SKP, Woo PCY, Suen KY, Yuen KY, Guan Y, Peiris JSM. 2005. Identification of a novel coronavirus in bats. J Virol 79:2001–2009. https://doi.org/10.1128/jvi.79.4.2001-2009.2005.

31. Subudhi S, Rapin N, Bollinger TK, Hill JE, Donaldson ME, Davy CM, Warnecke L, Turner JM, Kyle CJ, Willis CKR, Misra V. 2017. A persistently infecting coronavirus in hibernating Myotis lucifugus, the North American little brown bat. J Gen Virol 98:2297–2309. https://doi.org/10.1099/jgv.0.000898.

32. Ding S, Liang TJ. 2020. Is SARS-CoV-2 Also an Enteric Pathogen With Potential Fecal–Oral Transmission? A COVID-19 Virological and Clinical Review. Gastroenterology 159:53–61. https://doi.org/10.1053/j.gastro.2020.04.052.

33. Saif LJ, Jung K. 2020. Comparative pathogenesis of bovine and porcine respiratory coronaviruses in the animal host species and SARS-CoV-2 in humans. J Clin Microbiol 58:e01355-20. https://doi.org/10.1128/jcm.01355-20.

34. Barthold SW, Beck DS, Smith AL. 1993. Enterotropic coronavirus (mouse hepatitis virus) in mice: influence of host age and strain on infection and disease. Lab Anim Sci 43:276–284. http://europepmc.org/abstract/MED/8231082.

35. Weiss SR, Leibowitz JL. 2011. Coronavirus pathogenesis. In Advances in Virus Research (Vol. 81, p 85–164). Academic Press Inc., New York, NY. https://doi.org/10.1016/B978-0-12-385885-6.00009-2.

36. Fehr AR, Perlman S. 2015. Coronaviruses: an overview of their replication and pathogenesis. In Coronaviruses: methods and Protocols p. 1–23. Springer, New York, NY. https://doi.org/10.1007/978-1-4939-2438-7_1.

37. Möstl K. 1990. Coronaviridae, pathogenetic and clinical aspects: an update. Comp Immunol Microbiol Infect Dis 13:169–180. https://doi.org/10.1016/0147-9571(90)90085-8.

38. Wang Q, Vlasova AN, Kenney SP, Saif LJ. 2019. Emerging and re-emerging coronaviruses in pigs. Curr Opin Virol 34:39–49. https://doi.org/10.1016/j.coviro.2018.12.001.

39. Murray J, Kiupel M, Maes RK. 2010. Ferret coronavirus-associated diseases. Vet Clin North Am Exot Anim Pract 13:543–560). https://doi.org/10.1016/j.cvex.2010.05.010.

40. Rottier PJM, Nakamura K, Schellen P, Volders H, Haijema BJ. 2005. Acquisition of macrophage tropism during the pathogenesis of feline infectious peritonitis is determined by mutations in the feline coronavirus spike protein. J Virol 79:14122–14130. https://doi.org/10.1128/jvi.79.22.14122-14130.2005.

41. Hartmann K. 2005. Feline infectious peritonitis. Vet Clin Small Anim 35: 39–79. https://doi.org/10.1016/j.cvsm.2004.10.011.

42. Plowright RK, Parrish CR, McCallum H, Hudson PJ, Ko AI, Graham AL, Lloyd-Smith JO. 2017. Pathways to zoonotic spillover. Nat Rev Microbiol 15:502–510. https://doi.org/10.1038/nrmicro2017.45.

43. Lina PHC, Reinhold JO. 1997. Ruige dwergvleermuis Pipistrellus nathusii (Keyserling & Blasius, 1839). In: Limpens H, Mostert K, Bongers W. (ed.), Atlas van de Nederlandse vleermuizen. Onderzoek naar verspreiding en ecologie, p. 164–171. KNNV Uitgeverij, Zeist, Netherlands.

44. Annan A, Baldwin HJ, Corman VM, Klose SM, Owusu M, Nkrumah EE, Badu EK, Anti P, Agbenyega O, Meyer B, Oppong S, Sarkodie YA, Kalko EKV, Lina PHC, Godlevska EV, Reusken C, Seebens A, Gloza-Rausch F, Vallo P, Tschapka M, Drosten C, Drexler JF. 2013. Human betacoronavirus 2c EMC/2012-related viruses in bats, Ghana and Europe. Emerg Infect Dis 19:456–459. https://doi.org/10.3201/eid1903.121503.

45. Reusken CB, Lina PH, Pielaat A, de Vries A, Dam-Deisz C, Adema J, Drexler JF, Drosten C, Kooi EA. 2010. Circulation of group 2 coronaviruses in a bat species common to urban areas in western europe. Vector-Borne Zoonotic Dis 10:785–791. https://doi.org/10.1089/vbz.2009.0173.

46. Baggen J, Vanstreels E, Jansen S, Daelemans D. 2021. Cellular host factors for SARS-CoV-2 infection. Nat Microbiol 6:1219–1232. https://doi.org/10.1038/s41564-021-00958-0.

47. Nelli RK, Roth JA, Gimenez-Lirola LG. 2022. Distribution of coronavirus receptors in the swine respiratory and intestinal tract. Veterinary Sciences 9:500. https://doi.org/10.3390/vetsci9090500.

48. Widagdo W, Sooksawasdi Na Ayudhya S, Hundie GB, Haagmans BL. 2019. Host determinants of MERS-CoV transmission and pathogenesis. Viruses 11:280. https://doi.org/10.3390/v11030280.

49. Speranskaya AS, Artiushin IV, Samoilov AE, Korneenko EV, Khabudaev KV, Ilina EN, Yusefovich AP, Safonova MV, Dolgova AS, Gladkikh AS, Dedkov VG, Daszak P. 2023. Identification and genetic characterization of MERS-related coronavirus isolated from Nathusius' pipistrelle (Pipistrellus nathusii) near Zvenigorod (Moscow region, Russia). International Journal of Environmental Research and Public Health 20:3702. https://doi.org/10.3390/ijerph20043702.

50. Widagdo W, Begeman L, Schipper D, Run PRv, Cunningham AA, Kley N, Reusken CB, Haagmans BL, van den Brand JMA. 2017. Tissue distribution of the MERS-Coronavirus receptor in bats. Sci Rep 7. https://doi.org/10.1038/s41598-017-01290-6.

51. Erben L, Buonanno A. 2019. Detection and quantification of multiple RNA sequences using emerging ultrasensitive fluorescent in situ hybridization techniques. Current Protocols in Neuroscience 87:e63. https://doi.org/10.1002/cpns.63.

52. Cantini F, Niccoli L, Matarrese D, Nicastri E, Stobbione P, Goletti D. 2020. Baricitinib therapy in COVID-19: a pilot study on safety and clinical impact. J Infection 81:318–356. https://doi.org/10.1016/j.jinf.2020.04.017.

53. Cevik M, Tate M, Lloyd O, Maraolo AE, Schafers J, Ho A. 2021. SARS-CoV-2, SARS-CoV, and MERS-CoV viral load dynamics, duration of viral shedding, and infectiousness: a systematic review and meta-analysis. Lancet Microbe 2: e13–e22. https://doi.org/10.1016/S2666-5247(20)30172-5.

54. Wölfel R, Corman VM, Guggemos W, Seilmaier M, Zange S, Müller MA, Niemeyer D, Jones TC, Vollmar P, Rothe C, Hoelscher M, Bleicker T, Brünink S, Schneider J, Ehmann R, Zwirglmaier K, Drosten C, Wendtner C. 2020. Virological assessment of hospitalized patients with COVID-2019. Nature 581:465–469. https://doi.org/10.1038/s41586-020-2196-x.

55. van Kampen JJA, van de Vijver DAMC, Fraaij PLA, Haagmans BL, Lamers MM, Okba N, van den Akker JPC, Endeman H, Gommers DAMPJ, Cornelissen JJ, Hoek RAS, van der Eerden MM, Hesselink DA, Metselaar HJ, Verbon A, de Steenwinkel JEM, Aron GI, van Gorp ECM, van Boheemen S, Voermans JC, Boucher CAB, Molenkamp R, Koopmans MPG, Geurtsvankessel C, van der Eijk AA. 2021. Duration and key determinants of infectious virus shedding in hospitalized patients with coronavirus disease-2019 (COVID-19). Nat Commun 12: 267. https://doi.org/10.1038/s41467-020-20568-4.

56. Drexler JF, Corman VM, Drosten C. 2014. Ecology, evolution and classification of bat coronaviruses in the aftermath of SARS. Antiviral Res 101: 45–56. https://doi.org/10.1016/j.antiviral.2013.10.013.

57. Decaro N, Elia G, Campolo M, Desario C, Mari V, Radogna A, Colaianni ML, Cirone F, Tempesta M, Buonavoglia C. 2008. Detection of bovine

coronavirus using a TaqMan-based real-time RT-PCR assay. J Virological Methods 151:167–171. https://doi.org/10.1016/j.jviromet.2008.05.016.

58. Munster VJ, Baas C, Lexmond P, Waldenström J, Wallensten A, Fransson T, Rimmelzwaan GF, Beyer WEP, Schutten M, Olsen B, Osterhaus ADME, Fouchier RAM. 2007. Spatial, temporal, and species variation in prevalence of influenza a viruses in wild migratory birds. PLoS Pathog 3:e61–638. https://doi.org/10.1371/journal.ppat.0030061.

59. Walker FM, Williamson CHD, Sanchez DE, Sobek CJ, Chambers CL. 2016. Species from feces: order-wide identification of chiroptera from guano and other non-invasive genetic samples. PLoS One 11:e0162342. https://doi.org/10.1371/journal.pone.0162342.

60. Richard M, Kok A, de Meulder D, Bestebroer TM, Lamers MM, Okba NMA, Fentener van Vlissingen M, Rockx B, Haagmans BL, Koopmans MPG, Fouchier RAM, Herfst S. 2020. SARS-CoV-2 is transmitted via contact and via the air between ferrets. Nat Commun 11:3496. https://doi.org/10.1038/s41467-020-17367-2.

61. de Souza Luna LK, Heiser V, Regamey N, Panning M, Drexler JF, Mulangu S, Poon L, Baumgarte S, Haijema BJ, Kaiser L, Drosten C. 2007. Generic detection of coronaviruses and differentiation at the prototype strain level by reverse transcription-PCR and nonfluorescent low-density microarray. J Clin Microbiol 45:1049–1052. https://doi.org/10.1128/jcm.02426-06.